Supplemental Information:

Comparative Analysis of Metal Contaminants and Environmental Persistent Free Radicals in Indoor Dust from Urban and Rural Households.

Emily R. Halpern,[1] Steven Sharpe,[1] Killian MacFeely,[1] Peter Christ,[1] Lauren Heirty,[1] Christopher P. West,[1] Tuong Van Nguyen,[1] Satya S. Patra,[3] Brian H. Magnuson,[3] Brandon E. Boor,[3] Paige A. Thompson,[4] Laura J. Claxton,[4] Orit Herzberg,[5] Meghan Kalvey,[5] Margaret Shilling,[5] Karen E. Adolph,[5] Alexander Laskin[1,2] *

[1]Department of Chemistry, Purdue University, West Lafayette, IN, USA
[2]Department of Earth, Atmospheric, and Planetary Sciences, Purdue University, West Lafayette, IN, USA
[3]Lyles School of Civil and Construction Engineering, Purdue University, West Lafayette, IN, USA
[4]Department of Health and Kinesiology, Purdue University, West Lafayette, IN, USA
[5]Department of Psychology, New York University, New York City, NY, USA

Environmental Science: Advances

Manuscript VA-ART-12-2025-000477

Revised January 27th, 2025

Table of Contents:

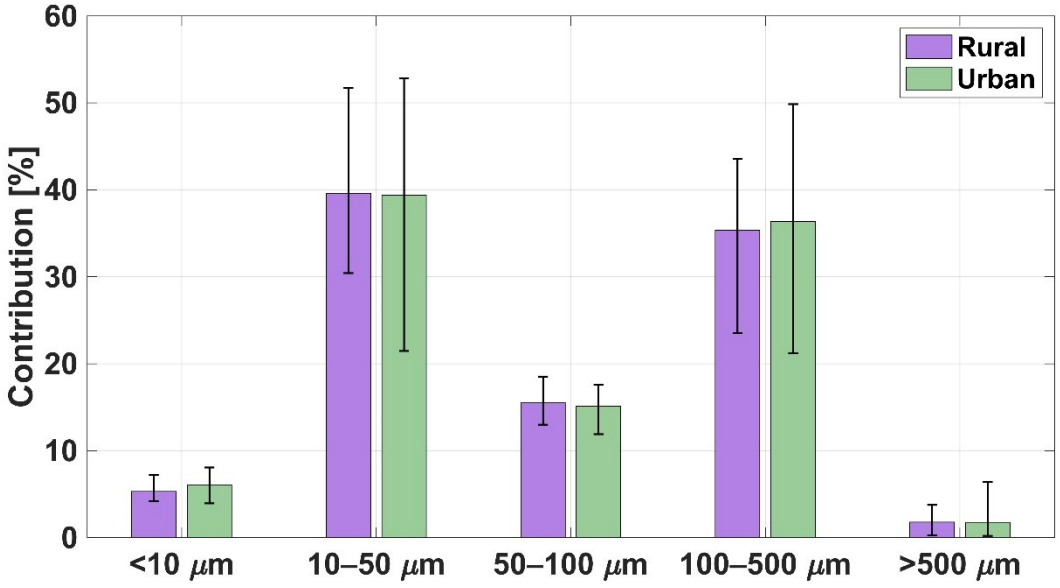

Figure S1. Size segregated volume fractions of dust from NYC (green) and WL (purple). The dust has two major size contributors, making up ~75% of the total dust volume (10-50 μm and 100-500 μm), and exhibits a bimodal distribution.

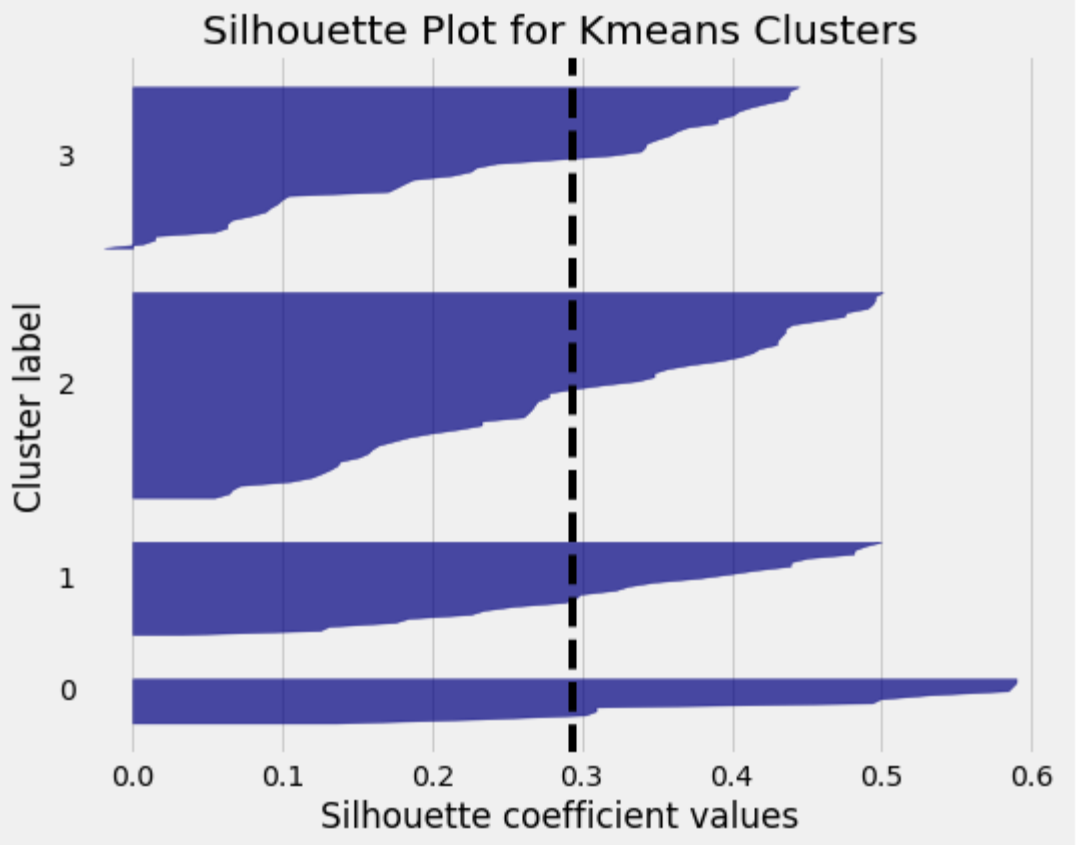

Figure S2. Silhouette coefficients for *k*-means dust-composition clusters. The silhouette value $s \in [-1,1]$ measures how much closer a sample is to its own cluster than to neighboring clusters; $s>0$ indicates better within-cluster cohesion than between-cluster proximity. As all clusters exhibit positive s, supporting internal coherence and meaningful separation.

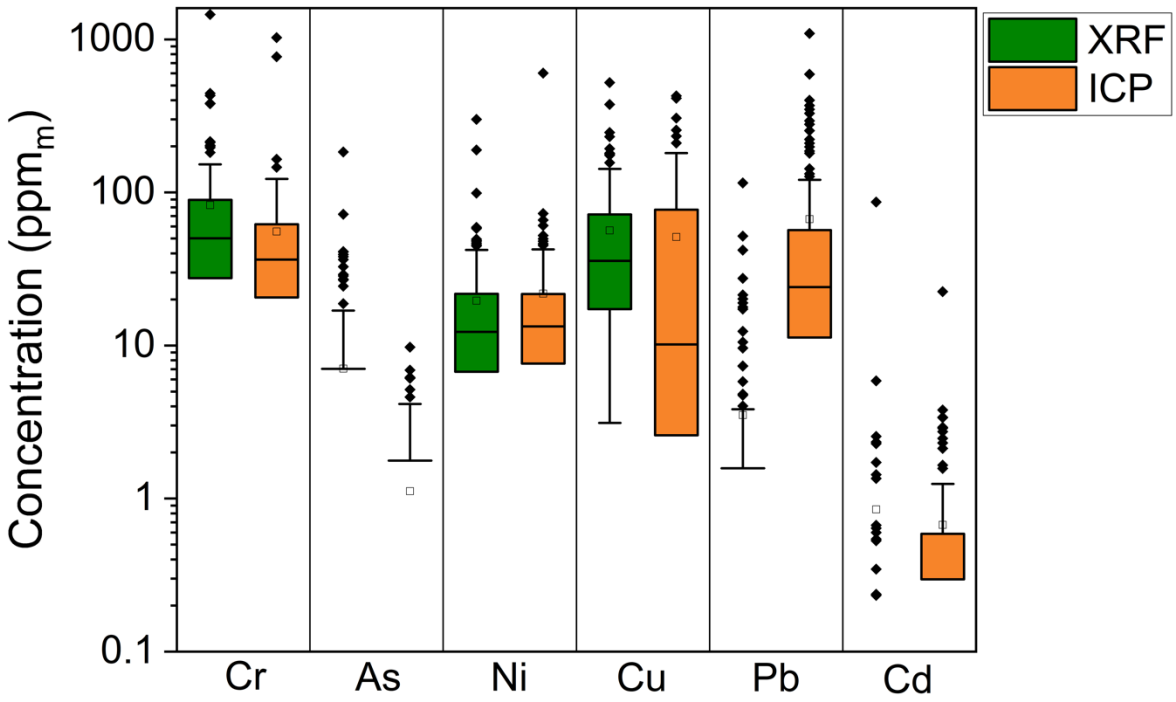

Figure S3. Box-and-whisker comparison of absolute metal concentrations in house dust measured by ICP-MS and estimated from XRF ratios. The central lines denote mean values; whiskers indicate the observed range. Across elements and samples, XRF-derived concentrations are generally within a factor of two of ICP-MS values, supporting the use of XRF ratio scaling for screening-level absolute quantitation.

Supplementary Note 1: Quality Assurance Protocols and Procedures

Dust Collection Controls and Procedures A vacuum cleaner with an aluminum nozzle and triple stitched vacuum bags was used to ensure consistent dust collection with a high-efficiency and low particle loss. Vacuum components were cleaned with isopropyl alcohol and inspected for defect before use. During collection the vacuum was held vertically, and dust was sealed in bags for transport. Method blanks were collected of the samples prior to analysis and video recordings were performed of the dust collection during the process. Validation of the protocol dust sample collection showed a 95% total mass recovery in laboratory environments.

XRF-related Procedures. A 4μm polypropylene foil (Prolene, Chemplex Industries, FL, USA) was used for sample measurement due to undetectable level of XRF-measured elements.[1] Before dust analysis was performed, a recalibration standard based on elements: Al, Ca, Fe, K, Mg, Na, P, S and Si was measured for drift correction in the soft X-ray region. After system-performed quantification, spectra were visually inspected for misassigned peaks and elements were removed or added as required before final quantification. The total dust sample was analyzed with this method, as it is nondestructive, resulting in a comprehensive measurement of all collected dust. Additionally, a triplicate measurement of dust elemental composition to examine homogeneity and reproducibility was taken and shown in Figure S4 below.

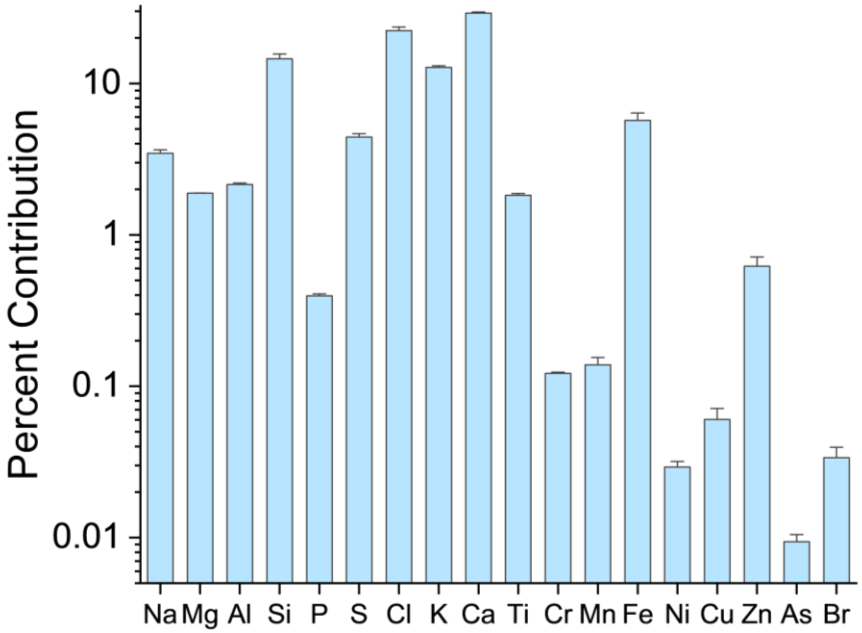

Figure S4. Triplicate replicates with represented error of XRF measurement of a dust sample, showing little deviation in determined percent contribution.

ICP-MS-related Procedures. Method blanks containing only water and nitric acid were prepared simultaneously with house dust samples and ran simultaneously. An external calibration curve was prepared for the ICP-MS runs containing Cr, Fe, Ni, Cu, Pb, As, and Cd. An internal In standard was used during experiments to further validate quantitation.

EPR spectroscopy-related Procedures. Before samples were measured for the day, a TEMPOL standard was measured to evaluate the radical signal/intensity ratio for the dust samples measured that day. Dust samples were mixed and dust was taken from all sections of the sample to be placed in the capillary to ensure a comprehensive measurement. All capillaries and EPR tubes were wiped before insertion into the instrument to avoid contamination between samples. The microwave cavity and bride were tuned before each sample was measured. Measurement of dust samples occurred prior to XRF experiments to ensure no impact by X-Ray beam on the dust samples.

Table S1. Summary of the average and median element concentrations included in Figure 2 from both urban and rural dust samples.

	Average Concentration (ppm_m)		Median Concentration (ppm_m)	
	Urban	Rural	Urban	Rural
Ca	3.5E+04	6.3E+04	2.4E+04	5.6E+04
Si	2.6E+04	9.0E+04	1.8E+04	5.8E+04
Cl	2.3E+04	5.6E+04	1.6E+04	3.0E+04
K	1.2E+04	1.8E+04	9.5E+03	1.5E+04
S	1.1E+04	1.9E+04	7.8E+03	1.2E+04
Na	1.1E+04	4.3E+04	6.4E+03	1.8E+04
Al	4.7E+03	1.8E+04	3.7E+03	1.1E+04
Fe	3.7E+03	4.6E+03	3.1E+03	3.8E+03
Mg	3.3E+03	1.0E+04	2.1E+03	5.2E+03
Ti	2.3E+03	2.4E+03	1.8E+03	2.1E+03
P	1.7E+03	4.6E+03	1.2E+03	3.4E+03
Zn	4.3E+02	2.6E+02	3.6E+02	1.8E+02
Pb	1.0E+02	3.9E+01	3.7E+01	1.3E+01
Cu	7.4E+01	5.5E+01	4.3E+01	3.3E+01
Mn	7.0E+01	1.2E+02	5.1E+01	1.0E+02
Cr	4.4E+01	6.5E+01	3.7E+01	3.6E+01
V	1.8E+01	2.2E+01	3.9E+00	8.9E-01
Zr	1.9E+01	2.1E+01	1.4E+01	1.6E+01
Ni	1.9E+01	2.5E+01	1.5E+01	1.3E+01
Sr	1.0E+01	1.1E+01	7.4E+00	7.5E+00
Br	6.8E+00	1.6E+01	4.9E+00	6.2E+00
Sn	3.2E+00	3.6E+00	3.1E+00	2.8E+00
Rb	1.6E+00	1.7E+00	1.7E+00	1.4E+00
Cd	9.0E-01	4.8E-01	2.9E-01	3.0E-01
As	5.4E-01	1.6E+00	Below LOD	7.6E-01

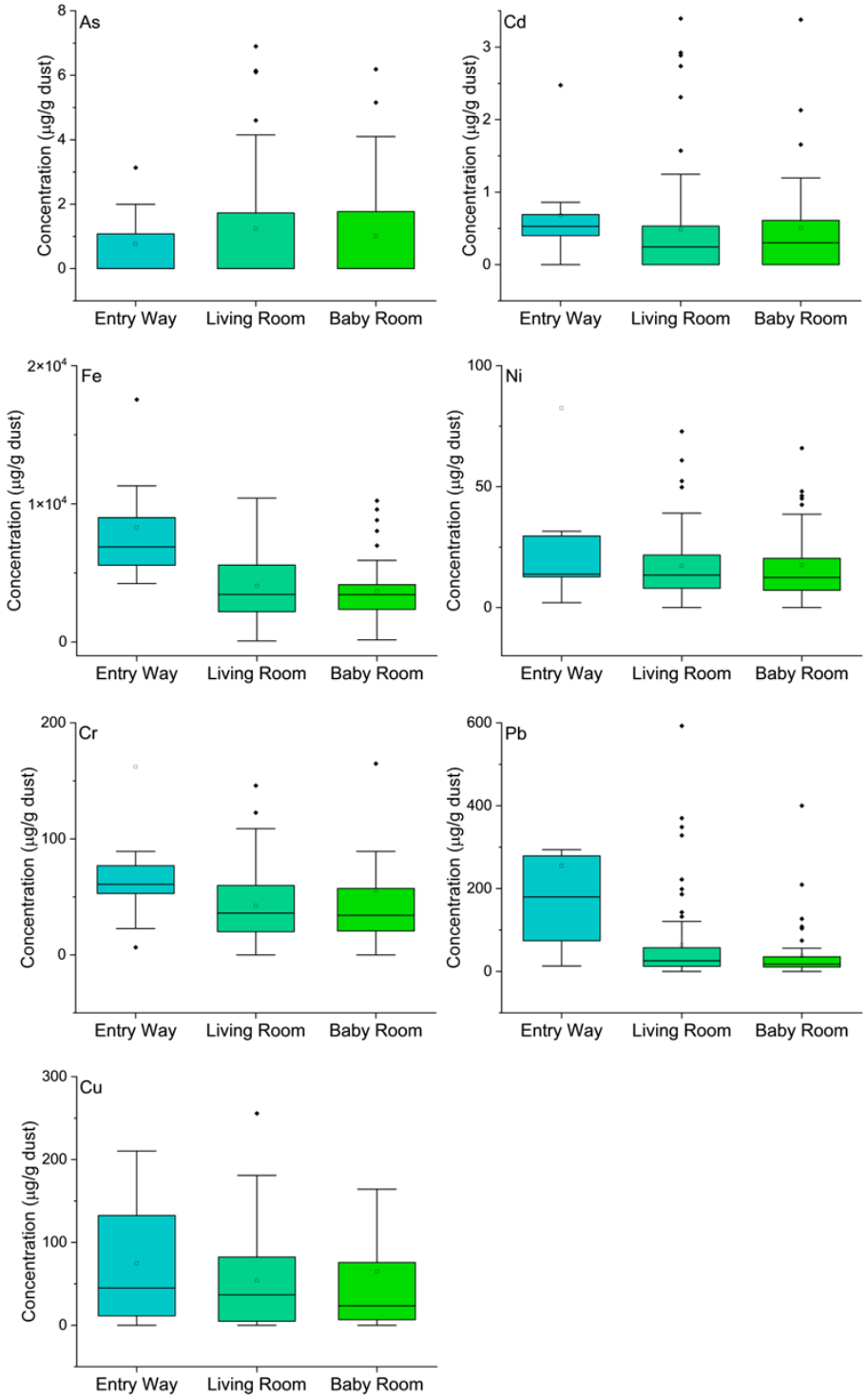

Figure S5. Distributions of toxic metal concentrations by room: entry way, living room, and infant bedroom. Elevated entryway levels for Fe, Pb, Cr, and Cd indicate likely outdoor tracking, whereas comparable levels of As, Ni, and Cu across rooms are consistent with indoor sources or broadly distributed emissions.

Table S2. Average and Median Enrichment Factor for each Element in Urban and Rural Regions

	Average Enrichment Factor		Median Enrichment Factor	
	Urban	Rural	Urban	Rural
Ca	13.7	16.3	9.9	11.6
Si	1.9	3.0	0.7	1.9
Cl	4035.7	5976.0	1864.9	2152.6
K	14.2	11.0	7.2	6.2
S	888.2	884.1	593.9	438.3
Na	10.4	32.0	4.3	6.5
Al	1.0	2.1	0.5	1.1
Fe	1.0	0.7	1.0	0.6
Mg	2.5	4.9	1.4	1.7
Ti	8.2	4.1	4.6	3.3
P	32.8	53.3	14.9	30.3
Zn	111.3	31.1	76.3	25.4
Pb	101.7	19.7	63.6	9.1
Cu	26.6	8.3	10.3	5.7
Cr	7.7	5.0	5.9	3.0
V	0.5	1.7	0.4	0.1
Zr	2.2	1.1	1.4	0.9
Ni	4.7	2.1	3.2	1.5
Sr	0.4	0.2	0.3	0.2
Br	50.2	74.8	38.2	23.8
Sn	33.8	27.6	24.4	14.1
Rb	0.3	0.1	0.3	0.2
Cd	91.4	22.4	20.7	8.9
As	5.8	6.8	Below LOD	5.0

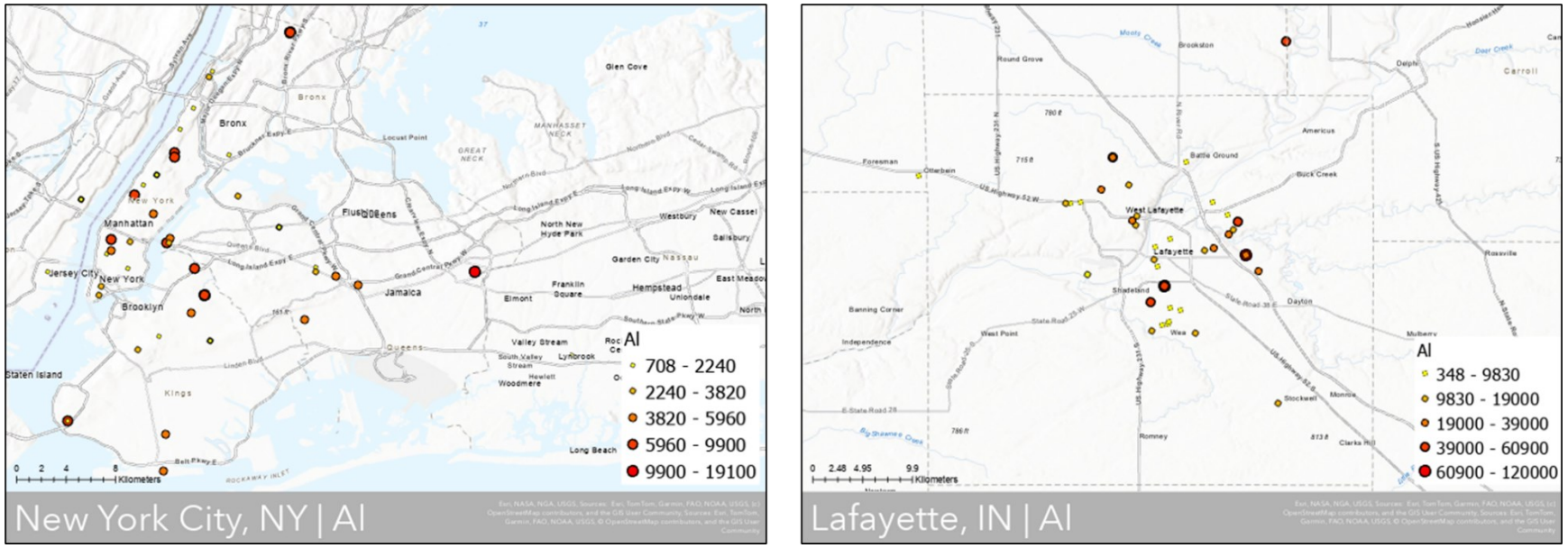

Figure S6. Spatial distribution of aluminum (Al) in house dust samples from NYC (left) and WL (right). Points mark sampling locations; fill intensity (darker red) scales with Al concentration (ppm_m). Both regions exhibit significant positive spatial autocorrelation (Moran's $I<0.05$), indicating clustered high-Al areas.

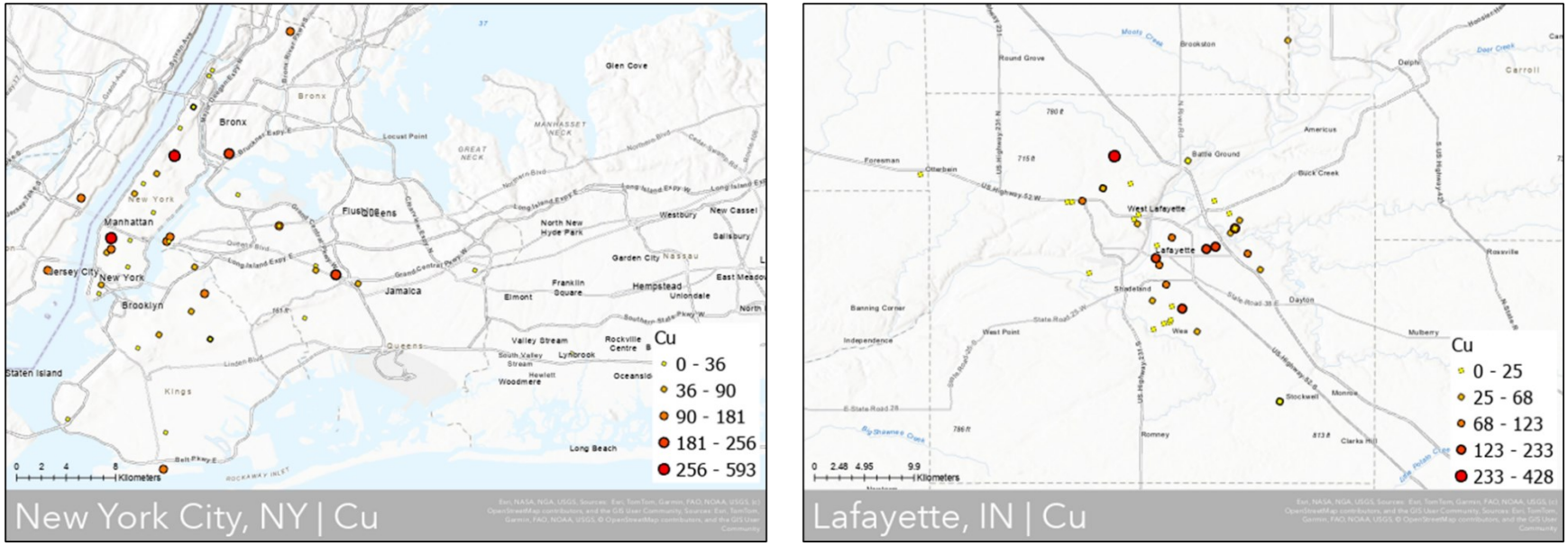

Figure S7. Spatial distribution of copper (Cu) in house dust samples from NYC (left) and WL (right). Points mark sampling locations; fill intensity (darker red) scales with Cu concentration (ppm_m). Only the rural samples exhibit significant positive spatial autocorrelation (Moran's $I<0.05$), indicating clustered high-Cu areas for the rural region.

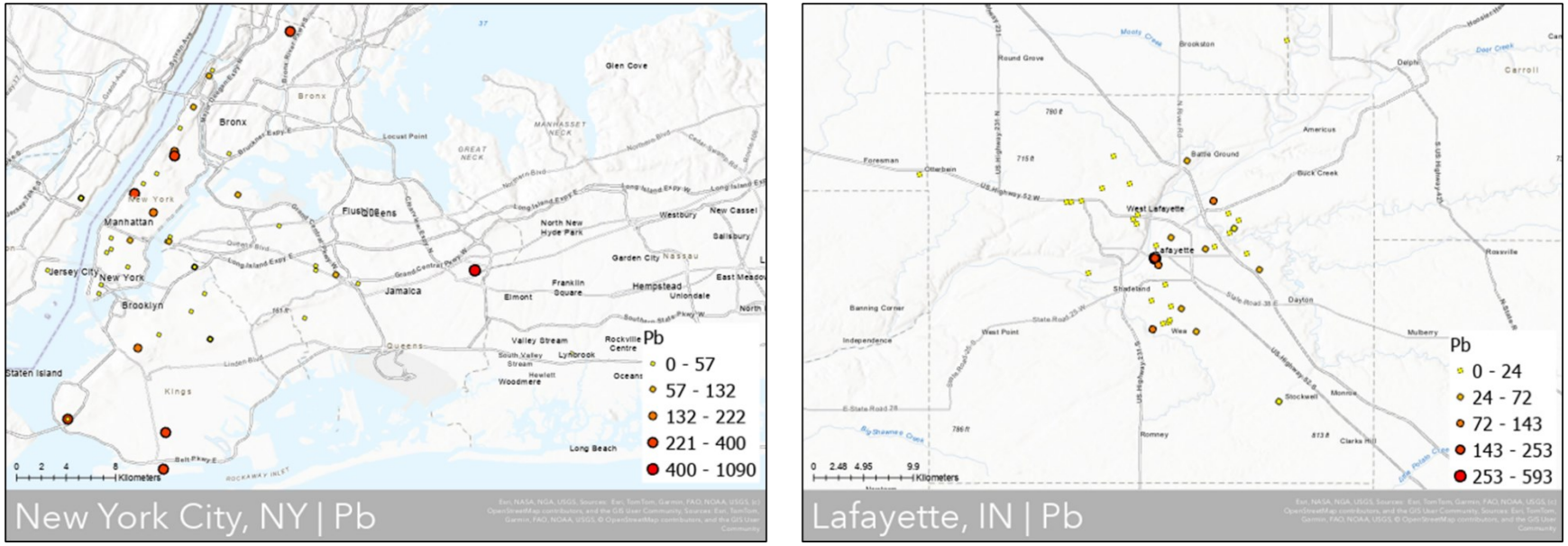

Figure S8. Spatial distribution of lead (Pb) in house dust samples from NYC (left) and WL (right). Points mark sampling locations; fill intensity (darker red) scales with Pb concentration (ppm_m). Only rural regions exhibit significant positive spatial autocorrelation (Moran's $I<0.05$), indicating clustered high-Pb rural areas.

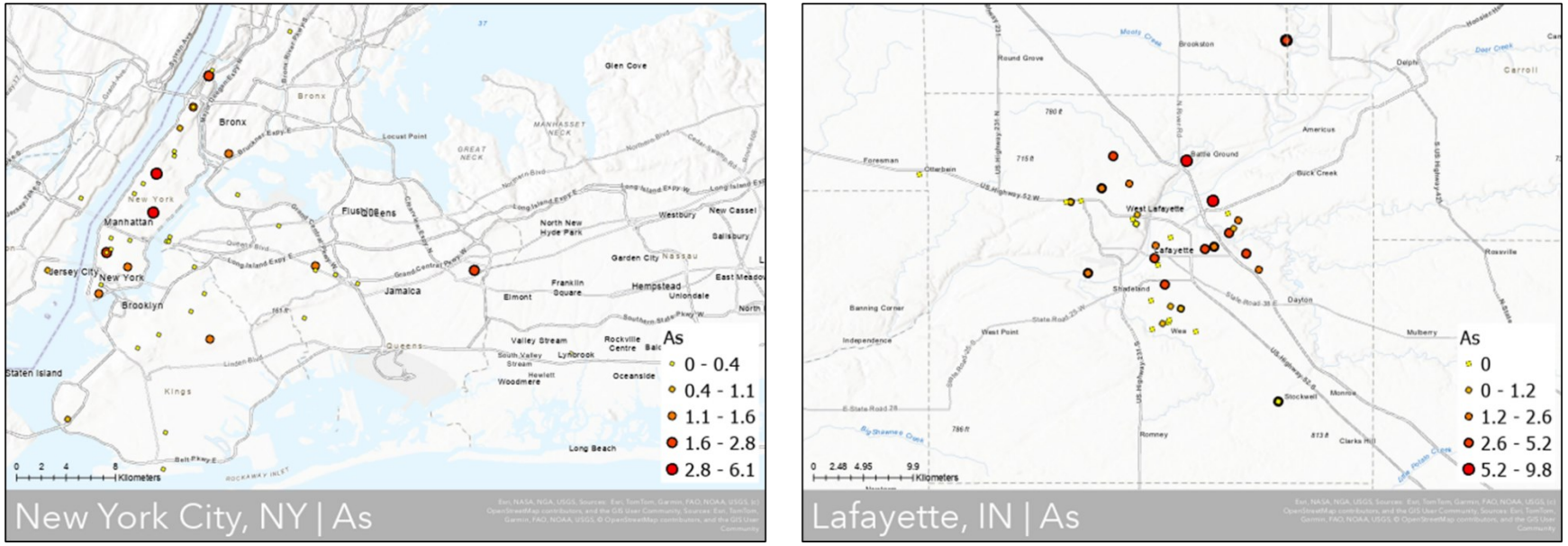

Figure S9. Spatial distribution of arsenic (As) in house dust samples from NYC (left) and WL (right). Points mark sampling locations; fill intensity (darker red) scales with As concentration (ppm_m). Only rural regions exhibit significant positive spatial autocorrelation (Moran's $I<0.05$), indicating clustered high-As rural areas.

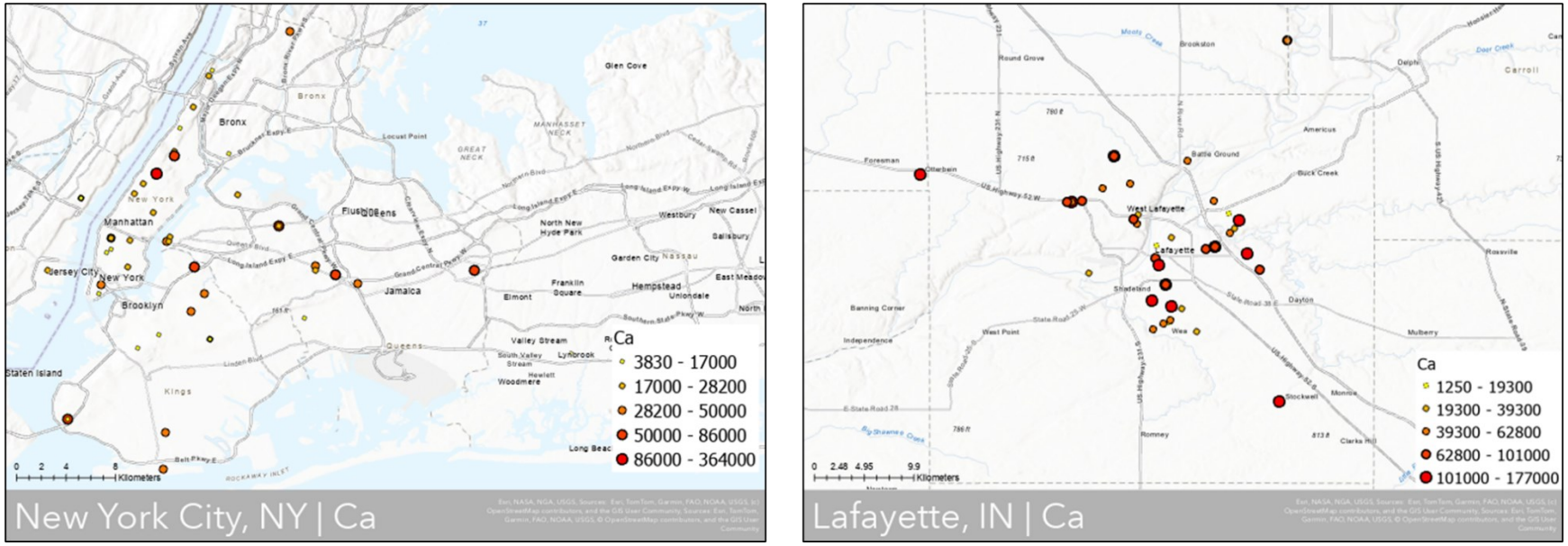

Figure S10. Spatial distribution of calcium (Ca) in house dust samples from NYC (left) and WL (right). Points mark sampling locations; fill intensity (darker red) scales with Ca concentration (ppm_m). Only rural regions exhibit significant positive spatial autocorrelation (Moran's $I<0.05$), indicating clustered high-Ca rural areas.

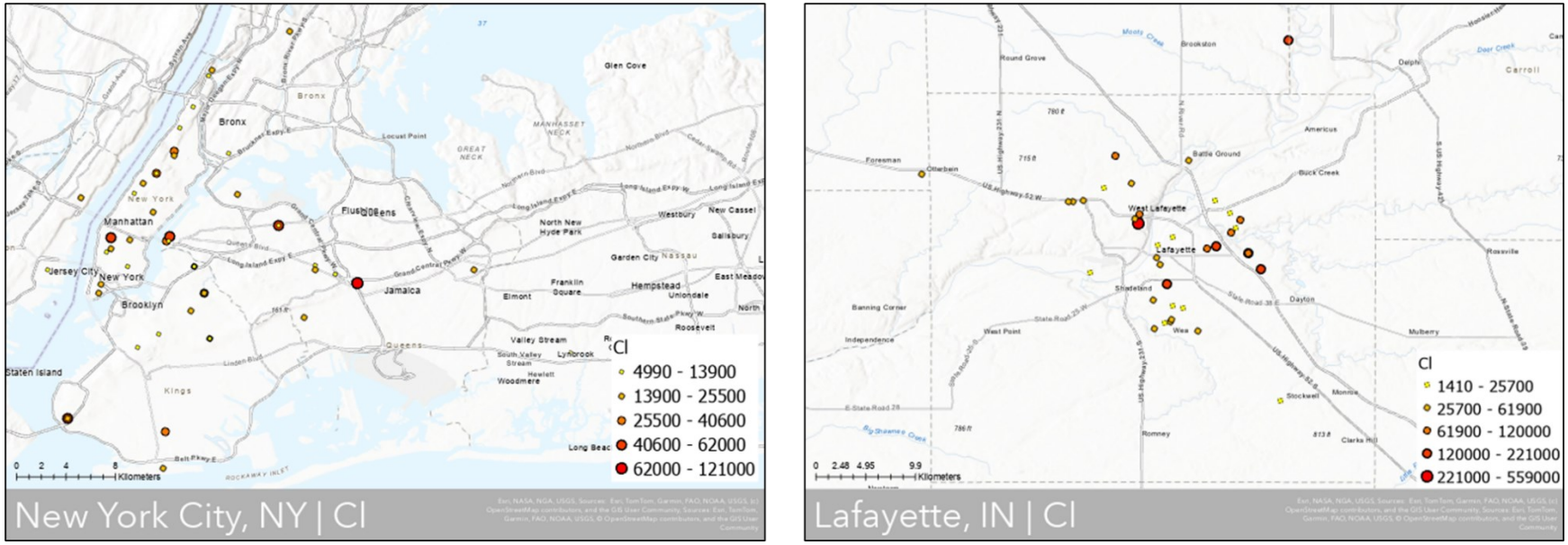

Figure S11. Spatial distribution of chlorine (Cl) in house dust samples from NYC (left) and WL (right). Points mark sampling locations; fill intensity (darker red) scales with Cl concentration (ppm_m). Both regions exhibit significant positive spatial autocorrelation (Moran's $I<0.05$), indicating clustered high-Cl areas.

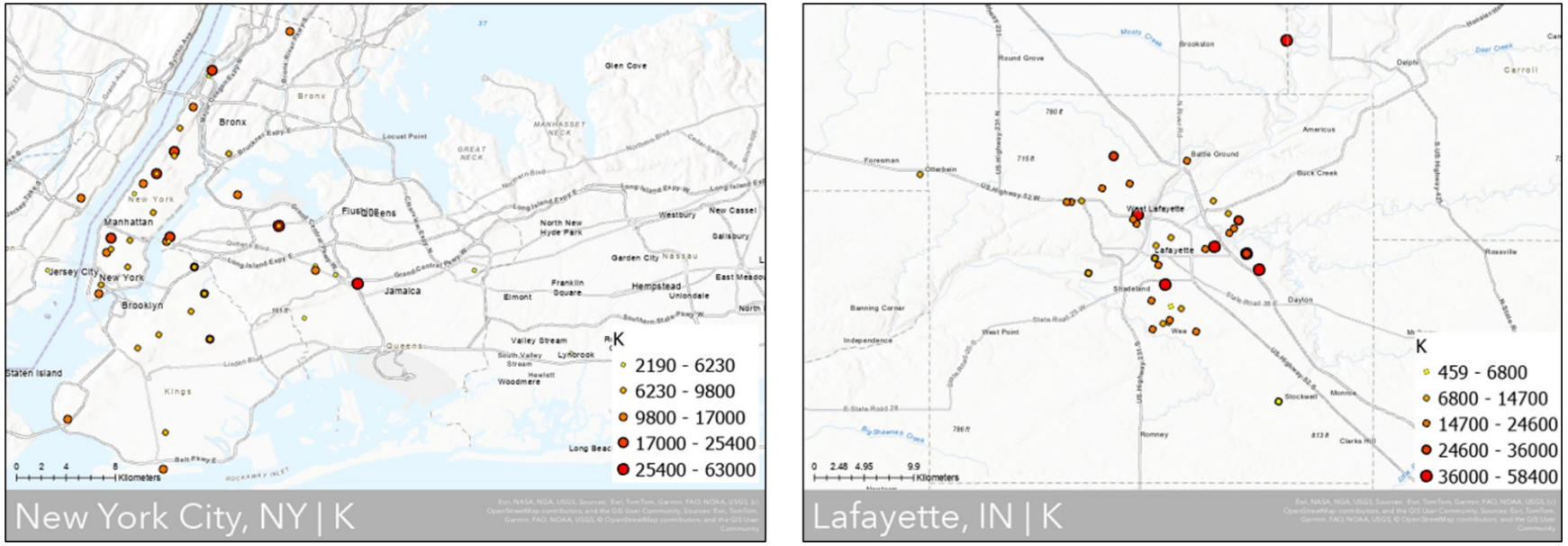

Figure S12. Spatial distribution of potassium (K) in house dust samples from NYC (left) and WL (right). Points mark sampling locations; fill intensity (darker red) scales with K concentration (ppm_m). Both regions exhibit significant positive spatial autocorrelation (Moran's $I<0.05$), indicating clustered high-K areas.

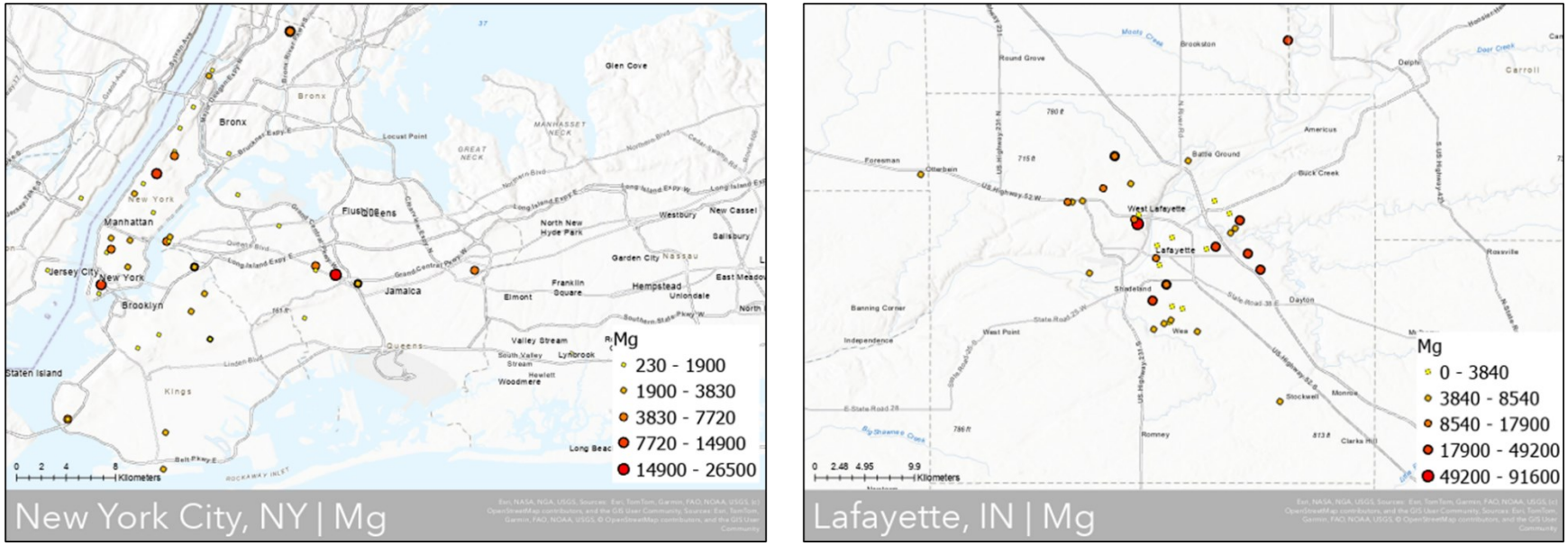

Figure S13. Spatial distribution of magnesium (Mg) in house dust samples from NYC (left) and WL (right). Points mark sampling locations; fill intensity (darker red) scales with Mg concentration (ppm_m). Only rural regions exhibit significant positive spatial autocorrelation (Moran's $I<0.05$), indicating clustered high-Mg rural areas.

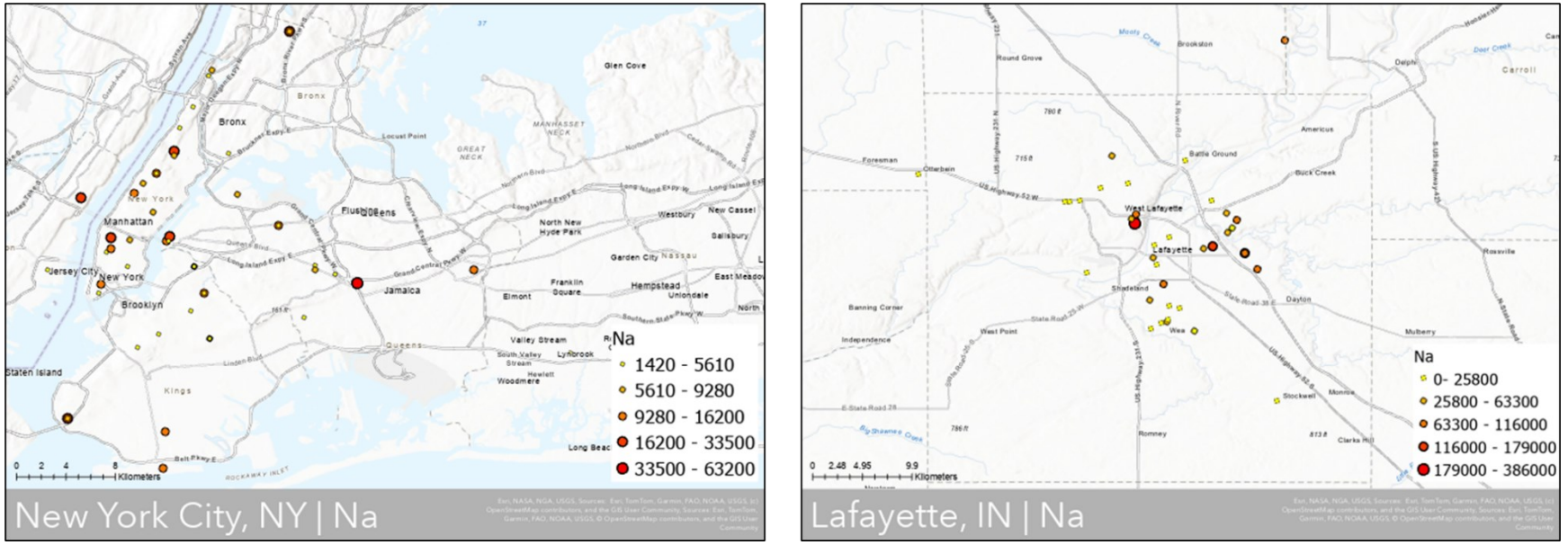

Figure S14. Spatial distribution of sodium (Na) in house dust samples from NYC (left) and WL (right). Points mark sampling locations; fill intensity (darker red) scales with Na concentration (ppm_m). Both regions exhibit significant positive spatial autocorrelation (Moran's $I<0.05$), indicating clustered high-Na areas.

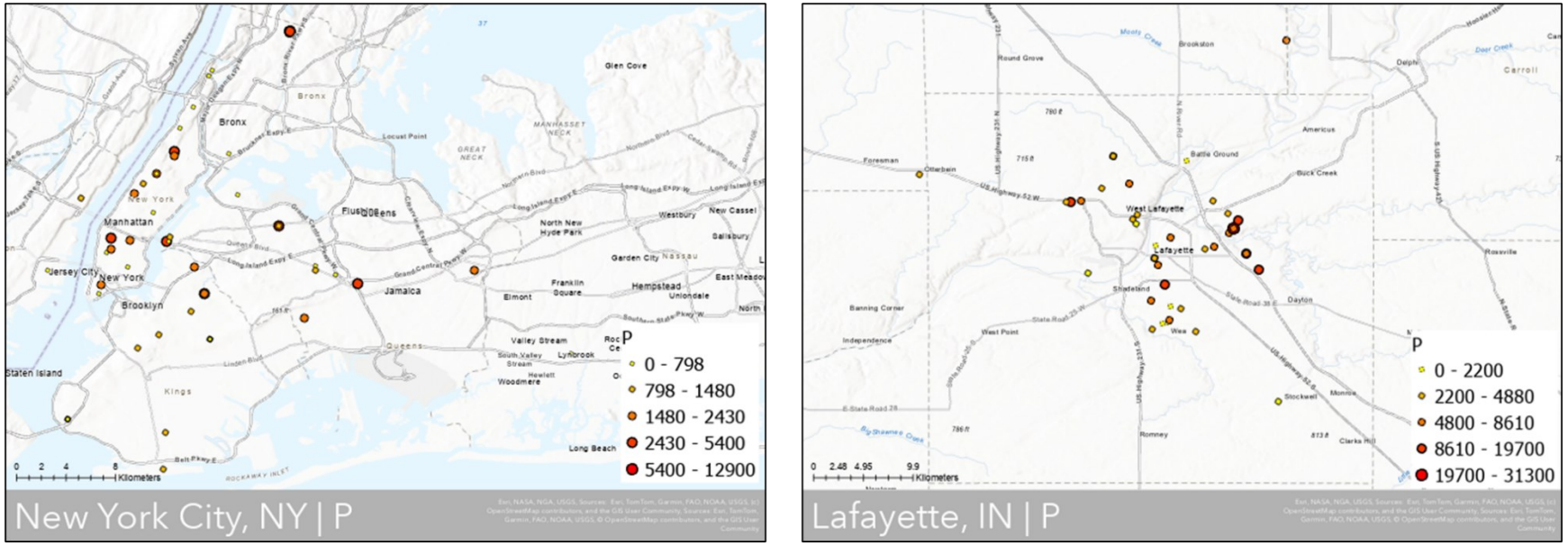

Figure S15. Spatial distribution of phosphorous (P) in house dust samples from NYC (left) and WL (right). Points mark sampling locations; fill intensity (darker red) scales with P concentration (ppm_m). Both regions exhibit significant positive spatial autocorrelation (Moran's I<0.05), indicating clustered high-P areas.

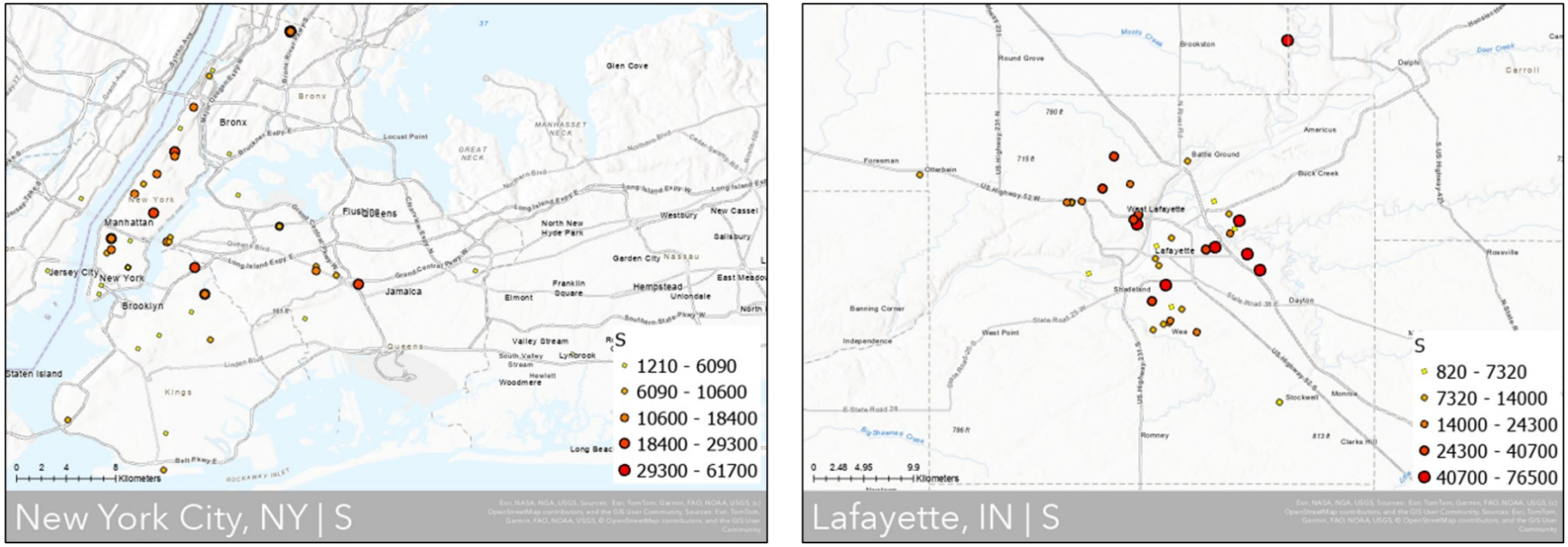

Figure S16. Spatial distribution of sulfur (S) in house dust samples from NYC (left) and WL (right). Points mark sampling locations; fill intensity (darker red) scales with S concentration (ppm_m). Both regions exhibit significant positive spatial autocorrelation (Moran's $I<0.05$), indicating clustered high-S areas.

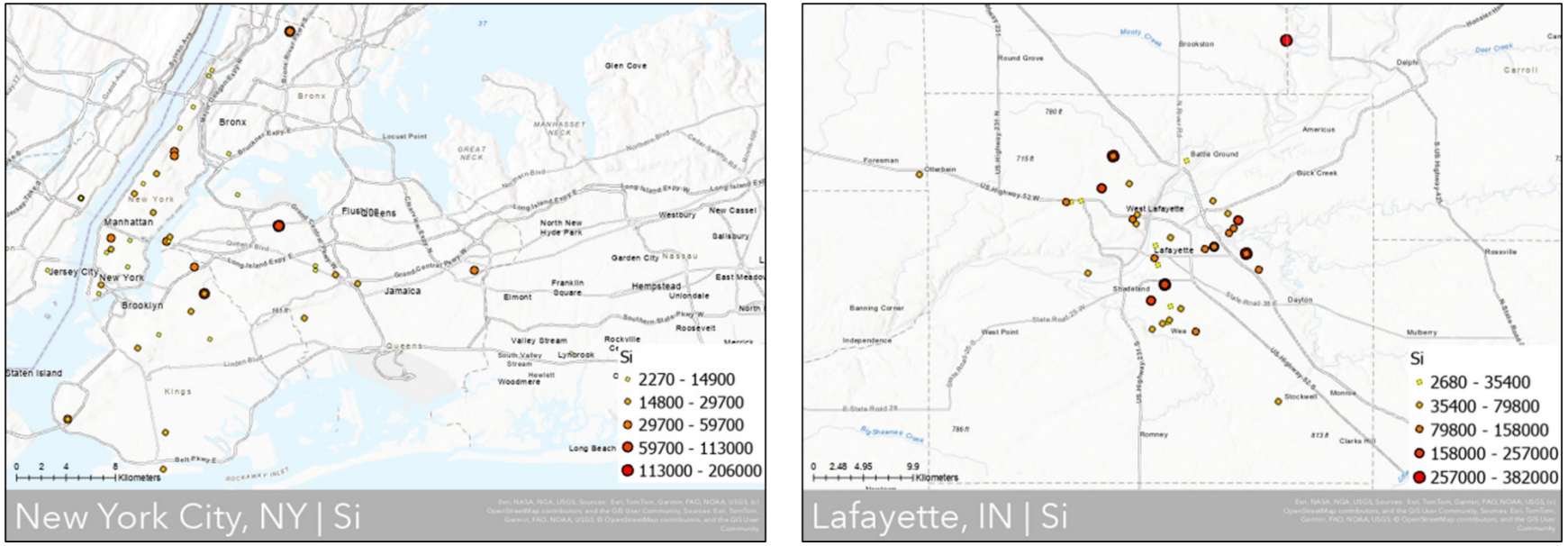

Figure S17. Spatial distribution of silicon (Si) in house dust samples from NYC (left) and WL (right). Points mark sampling locations; fill intensity (darker red) scales with Si concentration (ppm_m). Both regions exhibit significant positive spatial autocorrelation (Moran's $I<0.05$), indicating clustered high-Si areas.

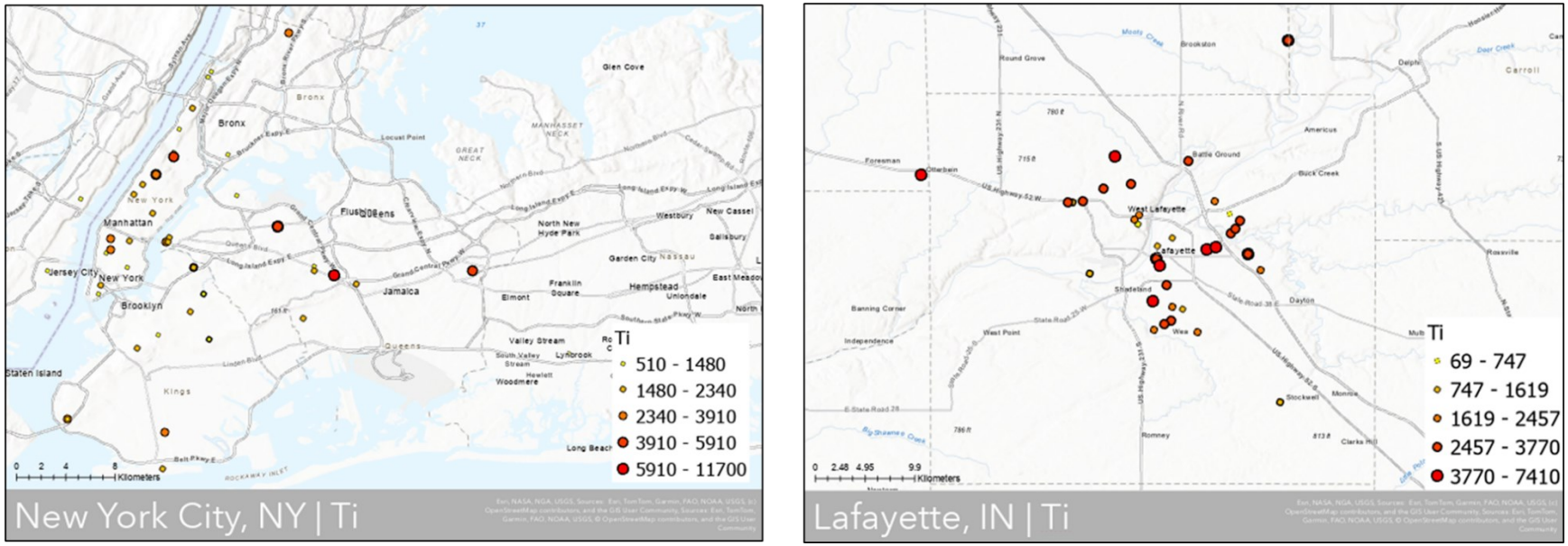

Figure S18. Spatial distribution of titanium (Ti) in house dust samples from NYC (left) and WL (right). Points mark sampling locations; fill intensity (darker red) scales with Ti concentration (ppm_m). Both regions exhibit significant positive spatial autocorrelation (Moran's $I<0.05$), indicating clustered high-Ti areas.

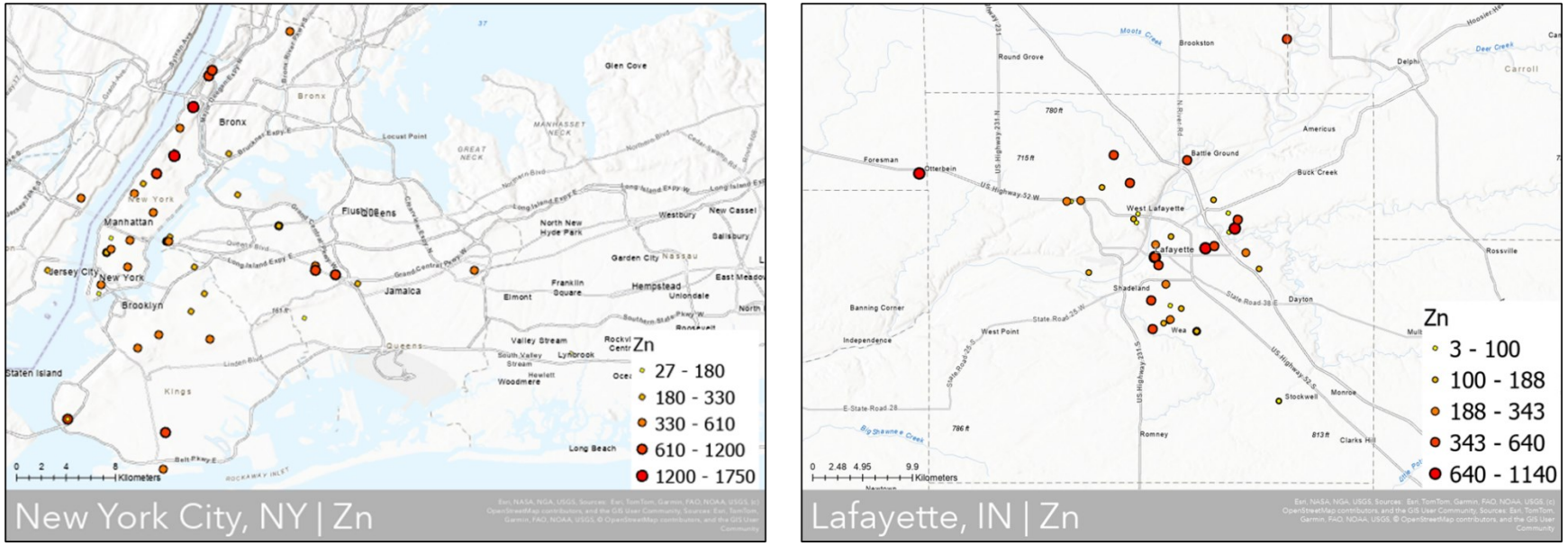

Figure S19. Spatial distribution of zinc (Zn) in house dust samples from NYC (left) and WL (right). Points mark sampling locations; fill intensity (darker red) scales with Zn concentration (ppm_m). Only rural regions exhibit significant positive spatial autocorrelation (Moran's $I<0.05$), indicating clustered high-Zn rural areas.

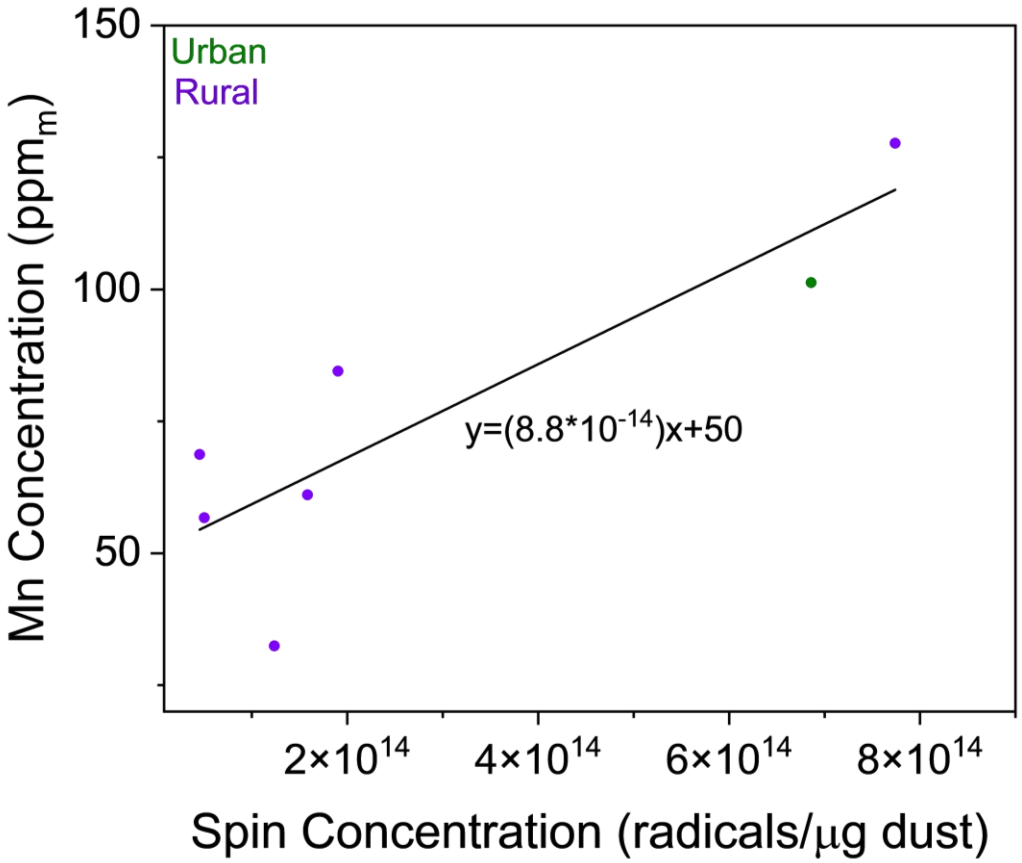

Figure S20. Correlation of Mn concentration to EPFR spin concentration from signal found in Figure 8c. There is a weak positive correlation between the concentration of the metal to the concentration of the Mn-formed signal.

Supplementary Note 2: Quantitative Estimates of Heavy Metal Toxicity Risk

Indications of dust toxicity can be determined by first determining an average daily dose (ADD, mg/kg/day) of heavy metals:

$$ADD = \frac{E * S_S}{BW} \; X \; 10^{-6} \qquad \text{(Eq. S1)}$$

where E is the concentration (mass) of heavy metals in the dust (mg/g), BW is the average body weight of an infant (12 kg), and S_S is the average daily dust ingestion rate (~60 mg/day).[2,3] Hazard quotient (HQ) is then determined as follows:[4]

$$HQ = ADD/RfD \qquad \text{(Eq. S2)}$$

where RfD is the element specific reference dose set by the EPA.[4] An HQ value substantially greater than 1 indicates potential adverse health effects from dust exposure.

Lifetime cancer risk (LCR) is determined through the following equation for As, Cd, Cr, and Pb:[4]

$$LCR = ADD * SF \qquad \text{(Eq. S3)}$$

where SF is a toxicant metal specific cancer slope factor. For LCR, an element is of risk if its value is substantially greater than 10^{-4}.

Table S3. Tabulated Hazard Quotients and Lifetime Cancer Risk Values for Average Concentrations of Toxic Metals from Urban and Rural Areas

Element	Type	Urban	Rural
Al	HQ	0.02	0.09
As	HQ	0.01	0.03
Cd	HQ	0.00	0.00
Cr	HQ	0.07	0.11
Cu	HQ	0.01	0.01
Fe	HQ	0.03	0.03
Ni	HQ	0.00	0.01
Pb	HQ	0.14	0.06
Zn	HQ	0.01	0.00
As	LCR	4.1E-06	1.2E-05
Cd	LCR	2.8E-05	1.5E-05
Cr	LCR	1.1E-04	1.6E-04
Pb	LCR	4.3E-05	1.7E-05

References:

(1) Zambito, J. J.; Haas, L. D.; Parsen, M. J. A Portable X-Ray Fluorescence (pXRF) Elemental Dataset Collected from Cambrian-Age Sandstone Aquifer Material, Wisconsin, U.S.A. *Data in Brief* **2022**, *43*, 108411. https://doi.org/10.1016/j.dib.2022.108411.

(2) Cohen, J.; Hubbard, H.; Özkaynak, H.; Thomas, K.; Phillips, L.; Tulve, N. Meta-Analysis of Soil and Dust Ingestion Studies. *Environmental Research* **2024**, *261*, 119649. https://doi.org/10.1016/j.envres.2024.119649.

(3) Hubbard, H.; Özkaynak, H.; Glen, G.; Cohen, J.; Thomas, K.; Phillips, L.; Tulve, N. Model-Based Predictions of Soil and Dust Ingestion Rates for U.S. Adults Using the Stochastic Human Exposure and Dose Simulation Soil and Dust Model. *Science of The Total Environment* **2022**, *846*, 157501. https://doi.org/10.1016/j.scitotenv.2022.157501.

(4) Tan, S. Y.; Praveena, S. M.; Abidin, E. Z.; Cheema, M. S. A Review of Heavy Metals in Indoor Dust and Its Human Health-Risk Implications. *Rev Environ Health* **2016**, *31* (4), 447–456. https://doi.org/10.1515/reveh-2016-0026.